JBMR Plus, 2024, **8**, ziae128
https://doi.org/10.1093/jbmrpl/ziae128
Advance access publication: October 10, 2024
Research Article

In nondiabetic C57BL/6J mice, canagliflozin affects the skeleton in a sex- and age-dependent manner

Carolyn Chlebek[1], Casey McAndrews[2], Samantha N. Costa[1,3], Victoria E. DeMambro[1,3], Shoshana Yakar[4], Clifford J. Rosen[1,3,5,*]

[1]Center for Molecular Medicine, MaineHealth Institute for Research, Scarborough, ME 04074, United States
[2]University of New England College of Osteopathic Medicine, Biddeford, ME 04005, United States
[3]Graduate School of Biomedical Sciences and Engineering, University of Maine, Orono, ME 04469, United States
[4]New York University College of Dentistry, New York, NY 10010, United States
[5]Tufts University School of Medicine, Tufts University, 136 Harrison Avenue, Boston, MA 02111, United States
*Corresponding author: Clifford J. Rosen, Center for Molecular Medicine, MaineHealth Institute for Research, 81 Research Drive, Scarborough, ME 04074, United States (cjrofen@gmail.com)

Abstract

Canagliflozin (CANA) is a sodium glucose cotransporter-2 inhibitor that reduces blood glucose levels. Sodium glucose cotransporter-2 is primarily expressed in the kidney, but not in any bone cells, therefore effects on the skeleton are likely to be non-cell autonomous. Originally developed to treat type II diabetes, CANA use has expanded to treat cardiovascular and renovascular disease. Clinical trials examining CANA in diabetic patients have produced contradictory reports on fracture risk, but there are limited data of CANA in nondiabetic conditions. In nondiabetic preclinical models, short-term treatment with CANA negatively affected trabecular bone whereas long-term treatment reduced cortical bone mineralization in male but not female mice. To investigate the skeletal effects of an intermediate period of CANA treatment, we treated male and female C57BL/6 J mice with CANA (180 ppm) for 6 months. Age at treatment initiation was also evaluated, with cohorts starting CANA prior to skeletal maturity (3-months-old) or in adulthood (6-months-old). Longitudinal assessments of bone mineral density revealed early benefits of CANA treatment in female mice. At euthanasia, both trabecular and cortical bone morphology were improved by CANA treatment in males and females. Bone formation was reduced at the endosteal surface. CANA decreased osteoblast number in male mice and bone marrow adiposity in females. Overall, more skeletal benefits were recorded in CANA-treated females than males. Urinary calcium output increased with CANA treatment, but parathyroid hormone was not changed. Despite reduced fasting blood glucose, body composition and whole-body metabolism were minimally changed by CANA treatment. For all outcome measures, limited differences were recorded based on age at treatment initiation. This study demonstrated that in nondiabetic C57BL/6 J mice, an intermediate period of CANA treatment improved bone morphology, but reduced osteoblast and bone marrow adipocyte number as well as serum procollagen type 1 N-terminal pro-peptide in a sex-specific manner.

Keywords: bone, canagliflozin, SGLT2i, kidney-bone crosstalk, glucose

Lay Summary

Sodium glucose cotransporter 2 inhibitors, like canagliflozin (CANA), are used to treat type II diabetes, but have recently been approved for treatment of cardiovascular and renovascular disease. There is concern that CANA may increase the risk of bone fracture in diabetic patients, but the findings are contradictory. Limited studies have examined skeletal health following CANA in nondiabetic models. In this study, we sought to determine the effects of an intermediate period of CANA treatment on male and female mice of varying skeletal maturity. We found that 6 months of CANA improved bone morphology in nondiabetic mice. Females gained more morphological benefits from CANA treatment than males. Bone marrow adiposity, which is often correlated with lower bone mass, was decreased by CANA treatment in females but not males. We also compared the age at initiation of CANA treatment; animals beginning treatment prior to skeletal maturity had similar responses to those treated in adulthood. In summary, intermediate periods of CANA improved bone morphology but reduced osteoblast and bone marrow adipocyte number.

Graphical Abstract

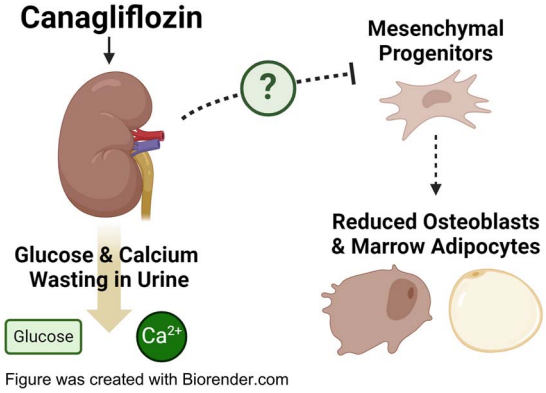

Figure was created with Biorender.com

Received: July 31, 2024. **Revised:** September 12, 2024. **Accepted:** October 4, 2024

Introduction

Canagliflozin (CANA) lowers serum glucose by inhibiting sodium glucose cotransporter 2 (SGLT2) in the kidney. SGLT2 is responsible for 90% of the reabsorption of glucose into the blood stream.[1] During SGLT2 inhibition, most glucose is not reabsorbed into the blood but instead is excreted into the urine, thereby lowering blood glucose levels. SGLT2 inhibitors (SGLT2i) were initially developed to treat type II diabetes but their indication has since been expanded to treat other conditions, including renal insufficiency and several types of heart failure; in addition to improved blood glucose levels, diabetic patients prescribed CANA had decreased blood pressure and lost weight.[2,3] In both diabetics and non-diabetics, SGLT2i markedly reduced cardiovascular risk decreased morbidity and mortality in congestive heart failure patients, and diminished time to progression of renal failure.[4] Monthly prescriptions of SGLT2i by cardiologists increased 12-fold following their indication for cardiovascular disease.[5] Clinically, SGLT2i are widely used, (i.e. 63.2 million prescriptions in the last 5 years[5]) and even have been studied for putative effects on lifespan.[6] Many patients begin SGLT2i therapy at midlife,[7] prior to periods of accelerated bone loss due to aging.[8]

Early clinical trials reported increased risk of bone fracture during CANA treatment,[9] but subsequent studies found no changes to fracture risk.[2,10–12] Expression of SGLT2 at both the gene and protein level occurs primarily in the proximal tubule of the kidney[13] and SGLT2 has not been detected in any bone cell, including osteoclasts, osteoblasts, and osteocytes.[14] Hence, bone is most likely affected in a non-cell autonomous manner by SGLT2 inhibition via systemic changes in calcium and glucose metabolism. Worsening of renal function has been linked to metabolic bone disease,[15] highlighting the importance of bone-kidney crosstalk. By preventing glucose and sodium reabsorption in the proximal tubule of the kidney, SGLT2i reduce serum glucose levels. SGLT2i also induce osmotic diuresis, which can lead to calcium wasting.[16] Reduced calcium levels can then increase parathyroid hormone (PTH) secretion.[17] In clinical studies, 5 days of CANA treatment increased PTH levels in humans[18] but had no effect on urinary calcium output.[19,20] Long-term effects of CANA on PTH in humans are currently unknown.[21] Limited studies have evaluated bone following SGLT2i in nondiabetic cohorts.[22,23] The expanded use of CANA combined with the history of contradictory findings for fracture risk highlights the need for investigation of bone quality following CANA treatment in nondiabetic models.

Length of CANA treatment elicits different skeletal effects in nondiabetic mice. Short-term treatment (2.5 months) with CANA negatively affected trabecular bone in the femur and vertebra of DBA/2 J mice[23] whereas long-term treatment (17 months) reduced femoral cortical mineralization in male but not female mice.[22] Intermediate treatment periods have not yet been examined. Further, the initiation of CANA treatment prior to accelerated trabecular bone loss versus in adulthood has not been compared. In this study, we hypothesized that CANA treatment would have skeletal impacts that were dependent on the sex and stage of development at treatment initiation. Additionally, we anticipated that the effects of CANA would be compartment-specific. Thus, we aimed to determine the effect of an intermediate period of CANA treatment on bone quality in nondiabetic C57BL/6 J mice, beginning CANA either prior to accelerated trabecular bone loss (3 months of age) or in adulthood (6 months of age).

Materials and methods

Mice

Male and female C57BL/6 J mice aged 3- or 6-months (Jackson Laboratories, Bar Harbor, ME) were randomly assigned to receive either CANA-containing (180 ppm[6,22]) or control diet for 6 months (Research Diets Inc, New Brunswick, NJ, $n = 10$/group). One month was defined as 4 weeks. Two animals were excluded for fighting, resulting in $n = 8$ for females beginning CANA treatment at 3-months of age. One mouse was euthanized prior to the end of the study due to a bad reaction to an injection, resulting in $n = 9$ for males receiving control diet starting at 3-months of age. Body weight measurements were obtained monthly. Following 6 months of treatment, at 9 or 12 months of age, mice were euthanized (Figure S1, See online supplementary material for a color version of this figure). Immediately prior to euthanasia, fasting blood glucose (6-hour fast with free access to water) was measured (AlphaTrak 2, Zoetis, Parsippany-Troy Hills, NJ).

All mouse procedures were performed under the approval of the Institutional Animal Care and Use Committee at the MaineHealth Institute for Research. Mice were group housed in 14-hour light:10-hour dark cycles during the study. Outside of fasting periods, all animals had ad libitum access to food and water.

Dual energy x-ray absorptiometry

Body mass, composition, bone mineral content (BMC), and bone mineral density (BMD) were assessed monthly in all animals using dual energy x-ray absorptiometry (Faxitron UltraFocus-DXA, Hologic, Marlborough, MA). The Faxitron was calibrated before each use with phantom standards provided by the manufacturer. A region of interest was selected to remove the mouse cranium from analysis. Areal bone mineral content, bone mineral density, fat mass, percent fat, and lean mass were calculated. Changes in body mass, composition, and BMD were calculated as the difference between final and baseline scans.

Indirect calorimetry

One week before euthanasia, eight animals from each group were housed individually in metabolic cages (Promethion cages, Sable Systems Intl., North Las Vegas, NV). All cages were equipped with standard bedding, a food hopper, water bottle, a house-like enrichment tube for body mass measurements, and 11.5 cm running wheel that recorded revolutions. Mice were allowed to acclimate for 24 hours prior to data collection. Following acclimation, data were assessed both over a 72-hour period and analyzed separately for day, night, and 24-hour cycles. Promethion Live software (v23.0.5) was used for data acquisition and instrument control, using previously published methods. Macro Interpreter (v22.10) was used to process the raw data. Respiratory quotient and energy expenditure were calculated by assessment of respiratory gases, using standard equations[24,25] (Promethion Core™ CCF, Sable Systems Intl.). Food and water intake were assessed. XYZ beam arrays (beam spacing of 0.25 cm) were used to monitor ambulatory activity and position of each mouse. To control for potential confounding factors associated with cage maintenance and data collection, animals were compared with their age- and sex-matched counterparts using t-tests.

Micro-computed tomography

Right femurs from all animals were collected for micro-computed tomography (μCT). Bones were fixed in 10% formalin and placed on a rocker for 24 hours before being rinsed, placed in 70% ethanol, and stored at 4°C. All bones were scanned using the same instrument under the same conditions, in accordance with the American Society for Bone and Mineral Research guidelines.[26] Using a high-resolution SkyScan micro-CT system (SkyScan 1172, Kontich, Belgium) with 10-MP digital detector, 10 W of energy (60 kV and 167 mA), and a pixel size of 9.7 microns, exposure 925 ms/frame rotation step 0.3 degrees with ×10 frame averaging, 0.5-mm aluminum filter (to increase the transmission), samples were scanned in the air with scan rotation of 180 degrees. Prior to morphometric analysis, global thresholding was applied. Image reconstructure was done using NRecon software (version 1.7.3.0; Bruker micro-CT, Kontich, Belgium). Data analysis was done using CTAn software (version 1.17.7.2+; Bruker micro-CT, Kontich, Belgium). 3D images were constructed using CT Vox software (version 3.3.0 r1403; Bruker micro-CT, Kontich, Belgium).

Dynamic histomorphometry

Prior to euthanasia (-10 days, -3 days), mice received calcein injections (10 mg/kg). Following μCT analysis, femurs from all animals were embedded in plastic and sectioned for dynamic histomorphometry. Cortical bone was sectioned in the transverse plane and trabecular bone was sectioned in the coronal plane. A single user calculated bone surface, single labels, and double labels in a blinded fashion. Measurements of mineral apposition rate, mineralized surface per bone surface (MS/BS), and bone formation rate (BFR/BS) were obtained for trabecular and cortical bone sections based on calcein labels using the OsteoMeasure (version 1.0.4.4, OsteoMetrics, Decatur, GA). For trabecular bone samples, the region of interest consisted of a 3×4 grid of 800×500 μm panels starting at the bottom of the growth plate, excluding anything within 200 μm of the cortical bone. The endosteal and periosteal surfaces of cortical bone were evaluated separately.

Histology and immunohistochemistry

One tibia from each animal was fixed in 10% formalin for 24 hours, then rinsed and stored in 70% ethanol. Bones were decalcified in 14% EDTA for 2 weeks. Half of the tibiae from each cohort ($n = 4$–5/group) were paraffin-embedded and sectioned sagittally at 5 μm thickness, then stained for hematoxylin and eosin, TRAP (Sigma-Adrich 387A), or anti pro-collagen-1 specific antibodies (Developmental Studies Hybridoma Bank SP1.D8). Bone marrow adiposity was evaluated using a region of interest beginning 200 μm below the growth plate and extending 3000 μm into the marrow cavity. Adiposity was quantified in ImageJ (version 2.14.0/1.54f) using hematoxylin and eosin-stained sections. Adipocyte number and size were averaged across three sequential sections per animal using previously established methods.[27] The number of bone-lining, cuboidal cells stained by procollagen-1 were quantified and normalized to bone surface. Metaphyseal cortical and trabecular bone were analyzed separately. Similarly, for osteoclast quantification, the number of tartrate-resistant acid phosphatase (TRAP)-positive cells was normalized to the bone surface and quantified separately for cortical and trabecular bone. Cortical bone was evaluated at the endocortical surface.

Serum collection and analysis

Blood was collection via cheek bleed at baseline. Following euthanasia, blood was also collected via cardiac puncture. Blood was stored at 8°C for 24 hours following collection. Samples were then centrifuged and serum was collected and stored at −80°C. Terminal CTx, procollagen type 1 N-terminal pro-peptide (P1NP), and insulin-like growth factor-1 (IGF-1) levels were measured by ELISA according to manufacturer's instructions (IDS AC-06F1, IDS AC-33f1, and ALPCO 22-IGF1MS-E01, respectively). Baseline and terminal measures of PTH were evaluated by ELISA in serum from young animals (Cloud-Clone Corp, CEA866Mu). Due to differences in total amount of serum obtained per animal, sample sizes of 5 – 10 were used for each ELISA.

Urine collection and analysis

Urine samples were collected at baseline and prior to euthanasia. Each urine collection period was 24 hours or less. Urine was collected into a 1.5 mL Eppendorf tube. Urine collection was attempted in all animals, but variability in animal compliance affected collection success. Every animal included in the analyses gave urine samples at least twice during the 24-hour period. Following collection, urine was centrifuged and stored at −80°C. Creatinine was diluted 1:50 and assessed using the manufacturer's instructions (Abcam ab204537). Similarly, calcium (1:2 dilution) and phosphate (1:2000 dilution) were evaluated in the urine (Abcam ab102505 and Abcam ab65622, respectively). Calcium and phosphate levels were normalized to creatinine.

Statistical analyses

Longitudinal data was analyzed using a two-way ANOVA with factors of drug and timepoint (bone mineral density, body mass, body composition, urine output, and PTH serum levels). The effect of "drug" refers to differences between CANA-treated and control mice for the cohort examined. The effect of "timepoint" refers to differences across timepoints examined. All four cohorts of mice were analyzed separately and Tukey's post-hoc tests determined significant differences between groups.

Data collected at a single timepoint was analyzed using a two-way ANOVA (bone morphology, dynamic histomorphometry, P1NP, osteoblast number, CTx, osteoclast number, marrow adiposity, and IGF-1). Factors of drug and developmental stage at treatment initiation (age effect) were examined. The effect of "drug" refers to differences between CANA-treated and control mice for the cohort examined. The effect of "age" refers to differences between mice starting treatment at 3-months versus 6-months of age. Males and females were analyzed separately and Tukey's post-hoc tests determined significant differences between groups. Similarly, differences between baseline and final measurements were analyzed using a two-way ANOVA with factors of drug and age.

For data collected from indirect calorimetry, treatment differences using age- and sex-matched controls were determined with t-tests.

In all tests, significance was set at $p < .05$. All statistical analyses were performed in R.

Results

Longitudinal measures of bone mineral density revealed early changes to the skeleton

Whole-body bone mineral content (aBMC) and density (aBMD) were evaluated monthly by DXA. Compared to age- and sex-matched controls, males starting CANA treatment at 3-months-of-age had greater areal aBMD (Figure 1A). In females, SGTL2 inhibition also increased aBMD (Figure 1B and D). A drug*timepoint interaction effect revealed differences in mineralization as early as 1-month post-treatment in young females. Despite the presence of a drug*timepoint interaction effect, Tukey post-hoc analyses revealed that at each timepoint examined, the aBMD of CANA-treated adult males was not significantly different from their age-matched controls (Figure 1C).

Changes in DXA-based bone parameters were calculated as the difference between baseline and final scans for each animal. In males, the change in aBMD and aBMC was not different between CANA-treated and control mice (Figure 1E). Isolated analysis of the femur revealed that adult males treated with CANA gained less aBMD over the course of the study compared to age-matched controls (drug*age interaction, p=.00616, data not shown). Adult male mice gained less aBMC during the study compared with their young counterparts (Figure 1E). In females, the change in aBMD and aBMC over six months of treatment was greater with CANA (Figure 1F). Similarly, femoral bone mineral density increased with CANA (p=.000304). Adult female mice gained less aBMC and aBMD compared to younger, sex-matched animals (Figure 1F).

Trabecular bone morphology was improved by CANA treatment but worsened with increasing age

Trabecular bone at the distal femur metaphysis was evaluated using micro-CT. Trabecular bone volume fraction and trabecular number were increased with CANA treatment in both sexes (Figure 2A and B, Table S1). CANA increased trabecular thickness in females, but not males (Figure 2C). Accordingly, CANA reduced trabecular separation in males (p=.000262, data not shown) but not females. Trabecular BMD increased with CANA treatment in males but not females (Figure 2D). CANA treatment had limited effects on dynamic histomorphometric indices in trabecular bone. In males, CANA treatment reduced trabecular mineralizing surface per bone surface (Figure 2E). The incidence of single- and double-labeled surfaces were also quantified with dynamic histomorphometry. CANA-treated females had more single-labeled trabecular surfaces compared to control animals. In trabecular bone, mineral apposition rate (Figure 2F) and bone formation rate were not changed with CANA treatment.

Trabecular bone morphology worsened with increasing age. Age decreased trabecular BMD in males. Males euthanized at 12 months had greater trabecular thickness and reduced trabecular separation compared with younger, sex-matched mice. Female mice aged 12 months at euthanasia had lower bone volume fraction, trabecular number, and bone mineral density compared with their younger sex-matched counterparts. As expected, trabecular separation increased with age in females.

Age also affected dynamic histomorphometry indices in trabecular bone. Males aged 12 months at euthanasia had lower trabecular mineral apposition rate and bone formation rate compared to their 9-month-old sex-matched counterparts. Compared to 9-month-old mice, 12-month-old females had lower trabecular mineral apposition rate but greater mineralizing surface per bone surface. A total of 12-month-old females also had fewer incidences of single- and double-labeled trabecular surfaces compared to 9-month-old mice.

Cortical bone morphology was improved by CANA treatment

In females, CANA increased cortical bone area and decreased marrow area (Figure 3A and B, Table S1). In males, CANA treatment reduced marrow area in adults but not young animals (Figure 3B). Similarly, cortical bone area fraction increased with CANA treatment in both ages in females, but only increased in adult males (Figure 3C). All CANA-treated animals had increased femoral cortical thickness compared with their age- and sex-matched controls (Figure 3D). CANA treatment increased polar moment of inertia in females but not males (Figure 3E). Similarly, maximum and minimum moments of inertia were also increased by CANA treatment in females but not males. Cortical bone mineral density was increased with CANA only in young females (Figure 3F).

Animal age also influenced cortical bone morphology. Males euthanized at 12 months of age had greater cortical area compared with their 9-month-old sex-matched counterparts. Cortical bone area fraction and cortical thickness decreased with age in females, but not males. Marrow area increased with age in female mice. In males receiving control diet, marrow area increased with age. In males, polar, maximum, and minimum moments of inertia were increased in older animals. Older male mice also had greater cortical BMD compared with their 9-month-old sex-matched counterparts. In females receiving a control diet, cortical BMD also was increased with age.

CANA treatment reduced endocortical bone formation in both growing and mature C57BL6 mice

In cortical bone, CANA affected endosteal but not periosteal bone formation rate. At the endosteal surface, CANA treatment reduced bone formation rate and mineral apposition rate in both male and female mice (Figure 4). CANA treatment reduced the endosteal mineralizing surface and the incidence of double labels in males but not females (Figure S2, See online supplementary material for a color version of this figure).

Age reduced endosteal mineral apposition rate in both sexes. 12-month-old males also had lower endosteal bone formation rates compared with their 9-month-old counterparts. Endosteal mineralizing surface and the incidence of double-labeled surfaces were increased with age in females. At the periosteal surface, mineralizing surface, bone formation rate, and the incidence of double-labeled surfaces were increased with age in males (Figure S3, See online supplementary material for a color version of this figure). In females, age reduced periosteal mineral apposition rate.

Systemic bone formation and osteoblast number were reduced by CANA treatment

Six months of CANA treatment reduced P1NP serum levels in females but not males (Figure 5A and B, See online supplementary material for a color version of this figure). P1NP did not differ between 9- and 12-month-old mice. In

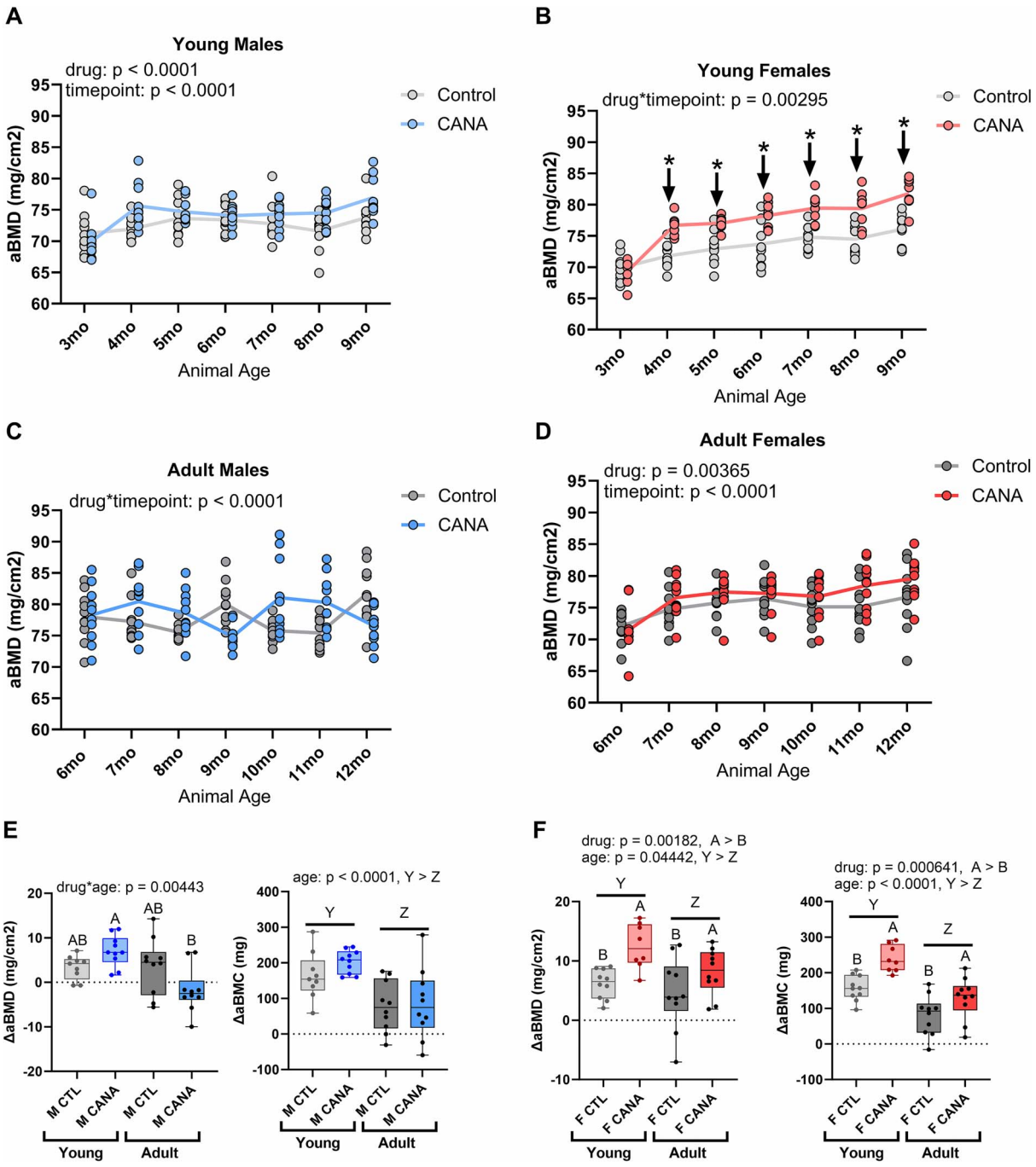

Figure 1. CANA increased bone mineral density in all females and in young males. Bone mineral density and content were evaluated in male and female mice once per month for 6 months. (A) CANA increased areal bone mineral density in young males (drug effect). Compared to baseline, aBMD was greater at every subsequent timepoint (timepoint effect). (B) Compared to control mice, young females treated with CANA had greater areal bone mineral density following 1 month of CANA treatment and at all subsequent timepoints (drug*timepoint interaction effect). The drug*timepoint significance with Tukey post-hoc analyses is indicated by *. Within the control group, compared to baseline measures, aBMD increased at 6 mo of age and was maintained at subsequent timepoints (drug*timepoint interaction effect). Within the CANA-treated mice, a significant increase in aBMD was recorded following one month of treatment (4 months of age) and again after 6 months of treatment (drug*timepoint interaction effect). (C) Bone mineral density was not altered by CANA in adult males. Tukey post-hoc analyses revealed that aBMD was not different between baseline and 12 months of age in control or CANA-treated adult male mice. Additionally, at each timepoint examined, there was no statistical difference between CANA-treated and control animals. (D) CANA increased areal bone mineral density in adult females (drug effect). Compared to baseline, aBMD was greater at every subsequent timepoint (timepoint effect). (E) the change in areal bone mineral density and bone mineral content over the course of the study was not different with CANA treatment in males. Males starting CANA at 3-months-of-age had a greater chance in aBMD compared to males starting CANA at 6-months-of-age. Across both control and CANA-treated males, the change in bone mineral content was greater in animals studied starting at 3-months-of-age versus 6-months-of-age. (F) CANA-treated females gained more aBMD and bone mineral content over the course of the study compared to control mice. Across both control and CANA-treated females, the change in aBMD and bone mineral content was greater in animals studied starting at 3-months-of-age versus 6-months-of-age. $p<.05$ for all effects displayed. The effect of "drug" refers to differences between CANA-treated and control mice for the cohort displayed. The effect of "timepoint" refers to differences across timepoints examined. The effect of "age" refers to differences between mice starting treatment at 3-months versus 6-months of age. A > B for CANA drug differences or drug*age interactions. Y > Z for age differences. Abbrevations: aBMD, whole-body bone mineral density; CANA. canagliflozin.

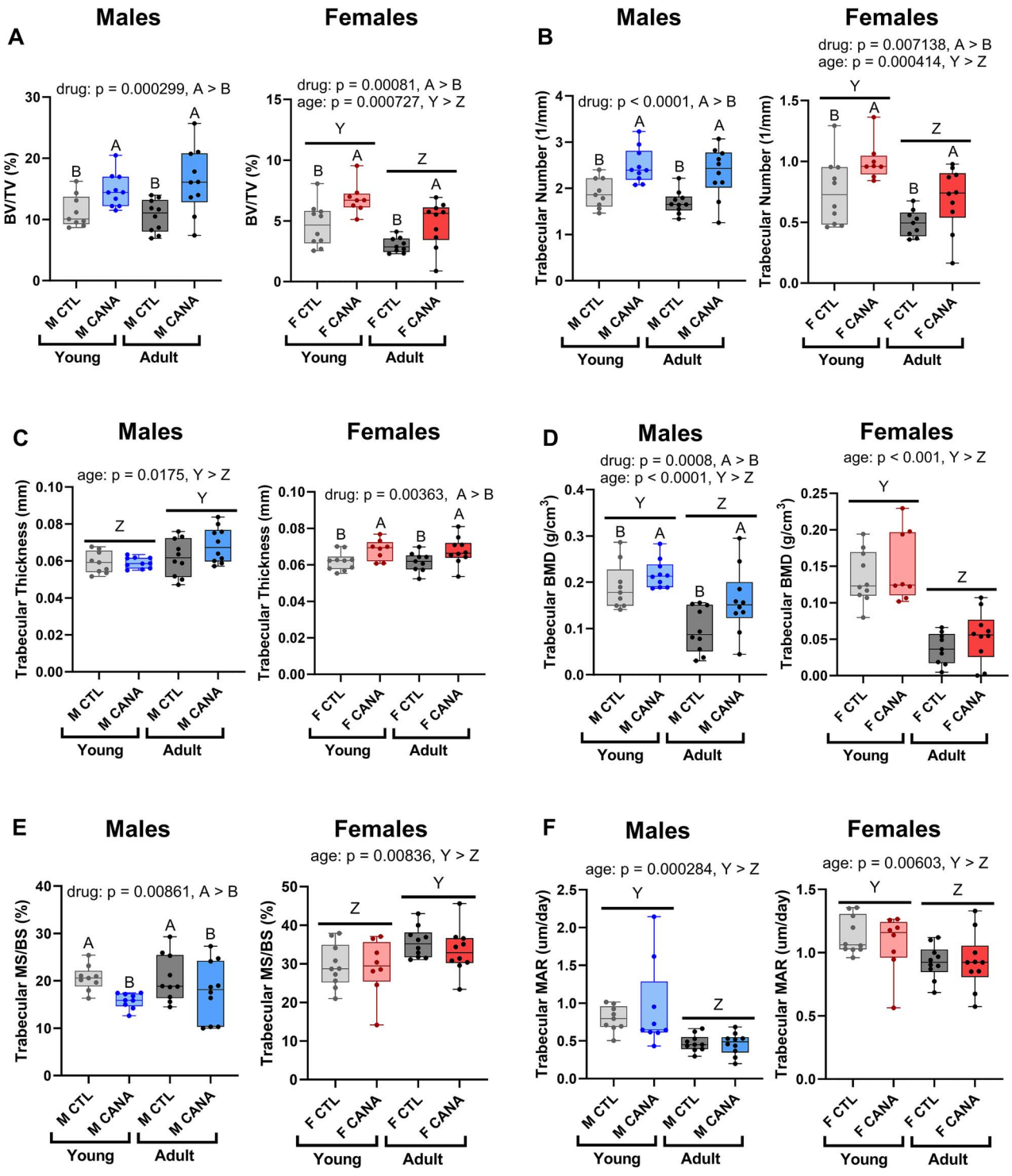

Figure 2. Trabecular bone morphology was improved with 6 months of CANA treatment. In both males and females, CANA increased (A) trabecular bone volume fraction and (B) trabecular number. (C) CANA-treated females had thicker trabeculae compared with control animals. (D) In male mice, CANA increased bone mineral density. (E) SGLT2 inhibition reduced trabecular mineralizing surface in males but not females. (F) CANA did not alter trabecular mineral apposition rate in either sex. $p<.05$ for all effects displayed. Compared to their 9-month-old counterparts, males aged 12-months at euthanasia had greater trabecular thickness (C), lower trabecular bone mineral density (D), and reduced trabecular mineral apposition rate (F). In males, age at euthanasia did not significantly affect bone volume fraction (A), trabecular number (B), nor trabecular mineralizing surface (E). Compared to their 9-month-old counterparts, females aged 12-months at euthanasia had less bone volume fraction (A), fewer trabeculae (B), lower trabecular bone mineral density (D), increased trabecular mineralizing surface (E), and decreased trabecular mineral apposition rate (F). In females, age at euthanasia did not significantly affect trabecular thickness (C). The effect of "drug" refers to differences between CANA-treated and control mice for the cohort displayed. The effect of "age" refers to differences between mice starting treatment at 3-months versus 6-months of age. A > B for CANA drug differences. Y > Z for age differences. Abbrevations: CANA, canagliflozin; SGLT2, sodium glucose cotransporter 2.

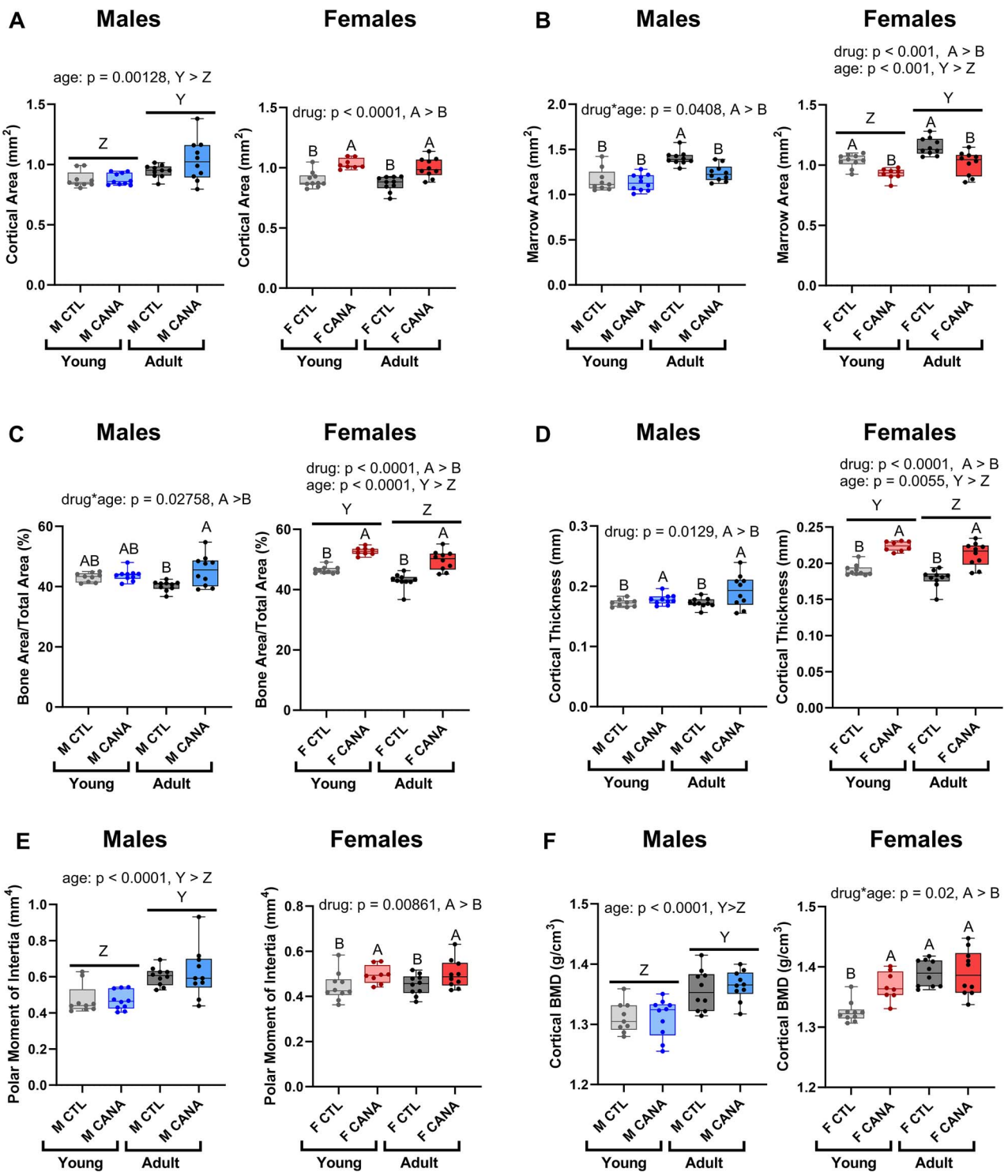

Figure 3. CANA improved cortical bone morphology in females more than males. (A) CANA treatment increased cortical bone area in females. Compared to their 9-month-old counterparts, males euthanized at 12-months-old had greater cortical area. (B) Marrow area was decreased with CANA in males starting treatment at 6 mo of age, but not 3 mo. All females treated with CANA had reduced marrow area. Compared to their 9-month-old counterparts, females euthanized at 12-months-old had greater marrow area. (C) In male mice, cortical bone volume fraction was increased with CANA treatment starting at 6 mo of age, but not 3 mo. Cortical bone volume fraction was increased with CANA treatment in females. Compared to their 9-month-old counterparts, females euthanized at 12-months-old had smaller cortical bone volume fraction. (D) CANA treatment increased cortical thickness in both sexes. Compared to their 9-month-old counterparts, females euthanized at 12-months-old had greater cortical thickness. (E) Polar moment of inertia was increased with CANA treatment in females. Compared to their 9-month-old counterparts, males euthanized at 12-months-old had greater polar moment of inertia. (F) Females starting CANA treatment at 3 mo had increased cortical bone mineral density compared to control animals. Compared to their 9-month-old counterparts, males euthanized at 12-months-old had greater cortical bone mineral density. $p<.05$ for all effects displayed. The effect of "drug" refers to differences between CANA-treated and control mice for the cohort displayed. The effect of "age" refers to differences between mice starting treatment at 3-months versus 6-months of age. A > B for CANA drug differences or drug*age interactions. Y > Z for age differences. Abbrevation: CANA, canagliflozin.

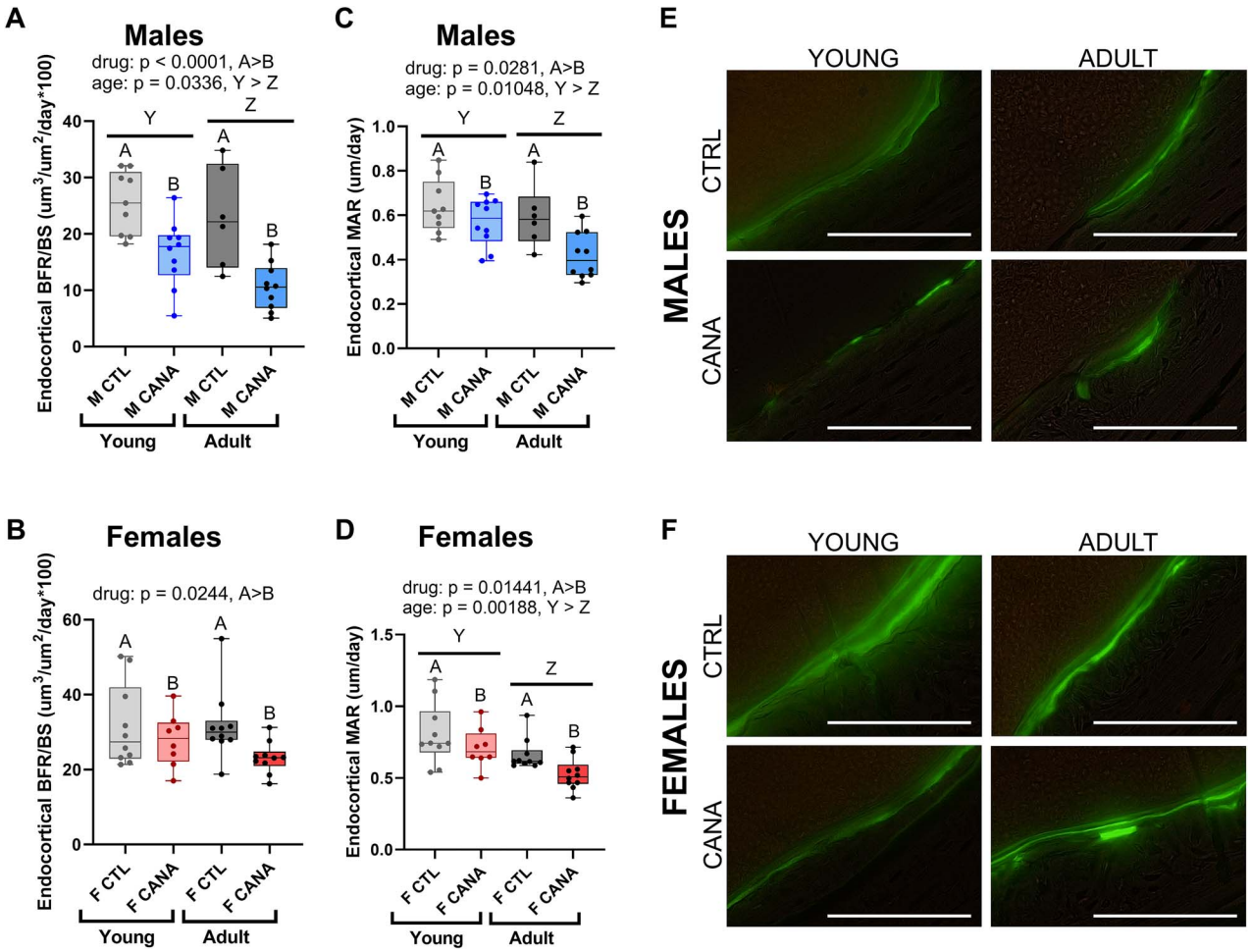

Figure 4. Endocortical bone formation was reduced by CANA treatment. (A-B) CANA reduced endocortical bone formation rate in both male and female mice. Compared to their 9-month-old counterparts, males euthanized at 12-months-old had smaller endocortical bone formation rate. (C-D) similarly, SGLT2 inhibition reduced endocortical mineral apposition rate in males and females. Compared to their 9-month-old counterparts, both males and females euthanized at 12-months-old had smaller endocortical mineral apposition rate. (E-F) representative images of endocortical surface labeled with calcein. Scale bar = 100um. $p<.05$ for all effects displayed. The effect of "drug" refers to differences between CANA-treated and control mice for the cohort displayed. The effect of "age" refers to differences between mice starting treatment at 3-months versus 6-months of age. A > B for CANA drug differences. Y > Z for age differences. Abbrevation: CANA, canagliflozin; SGLT2, sodium glucose cotransporter 2.

males beginning treatment at 3-months of age, CANA reduced osteoblast number in trabecular bone (Figure 5C and E). In control males, aging also reduced trabecular osteoblast number. Osteoblast number on the trabecular surface was not altered with treatment or age in females (Figure 5D and F). Osteoblast number on the endocortical surface of the cortical shell did not change with treatment or age in either sex.

Bone resorption and osteoclast number were not altered by CANA treatment

Serum crosslinked C-terminal telopeptides of type I collagen (CTx) was not different between treatment groups or ages in either sex (Figure S4A and B, See online supplementary material for a color version of this figure). Similarly, osteoclast number was not altered by CANA treatment or age at the tibial metaphyseal cortical shell. No age-related differences in osteoclast number were recorded in male trabecular bone (Figure S4C, See online supplementary material for a color version of this figure). In trabecular bone, females aged 12-months-old had more osteoclasts compared with their 9-month-old counterparts (Figure S4D, See online supplementary material for a color version of this figure.).

CANA reduced bone marrow adiposity in females

CANA reduced both the number and size of adipocytes in female mice (Fig. 6, p=.0337 and p=.00336, respectively). Similarly, the portion of area occupied by adipocytes was reduced CANA treatment in females (p=.0234). Bone marrow adiposity was not changed in CANA-treated male mice (Figure S5, See online supplementary material for a color version of this figure). Marrow adiposity was not statistically different between 9-month-old and 12-month-old mice.

CANA increased calcium excretion but did not alter IGF-1 or PTH levels

Urine was evaluated at baseline and prior to euthanasia. CANA treatment increased urinary calcium excretion in both sexes and ages (Figure S6, See online supplementary material for a color version of this figure). Phosphate excretion was not altered with CANA (Figure S7A, See online supplementary material for a color version of this figure). At euthanasia, CANA-treated animals had significantly lower creatinine levels in the urine compared with age- and sex-matched controls (Figure S7B, See online supplementary material for a color version of this figure). Food and water intake was evaluated

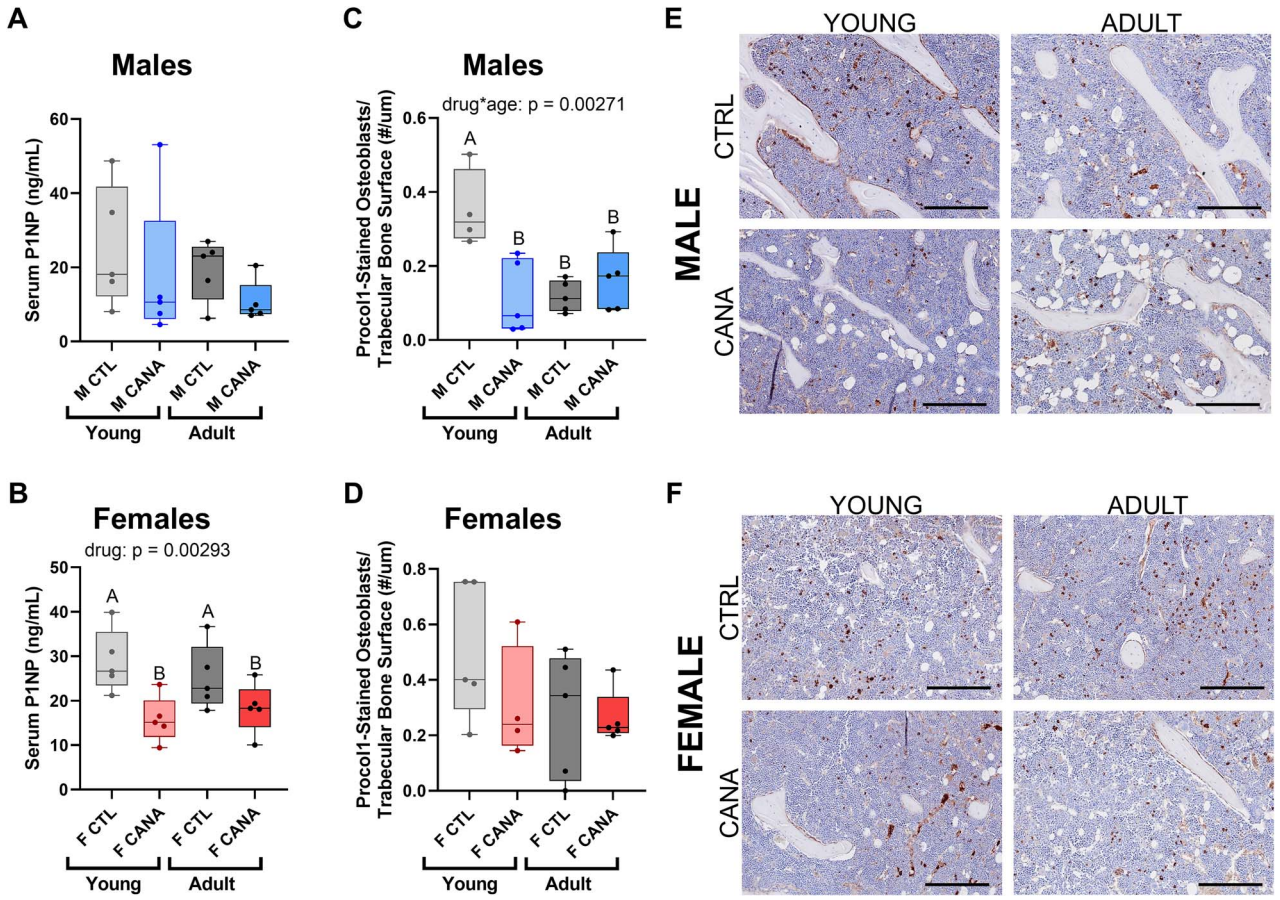

Figure 5. CANA reduced osteoblast number in males and P1NP levels in females. (A-B) CANA reduced serum P1NP in female, but not male, mice. Age at euthanasia did not affect serum P1NP. (C-D) trabecular osteoblast number was reduced by canagliflozin in males beginning treatment at 3-months-of-age. CANA treatment did not change osteoblast number in females or adult males. Age at euthanasia did not affect trabecular osteoblast number in females. (E-F) representative images of trabecular bone stained with procollagen-1. Scale bar = 200um. $p<.05$ for all effects displayed. The effect of "drug" refers to differences between CANA-treated and control mice for the cohort displayed. The effect of "age" refers to differences between mice starting treatment at 3-months versus 6-months of age. A > B for CANA drug differences or drug*age interactions. Abbrevation: CANA, canagliflozin; P1NP, procollagen type 1 N-terminal pro-peptide.

during the last week of the experiment, while mice were housed in metabolic cages; compared with sex- and age-matched controls, CANA-treated animals had greater water and food intake (Figure S8A and B, See online supplementary material for a color version of this figure). Based on food intake and bodyweight measurements, approximate dosing of CANA was calculated for each cohort (young males: 18.5 mg/kg, young females: 18.1 mg/kg, adult males: 20.3 mg/kg, adult females: 24.3 mg/kg).

IGF-1 was evaluated in the serum of all groups at euthanasia. In both males and females, serum IGF-1 was not changed by CANA treatment or animal age. PTH was evaluated at baseline and euthanasia in young animals. Serum PTH levels were not different with CANA treatment in young animals. Both male and female serum PTH levels were greater at euthanasia compared with baseline.

CANA had limited effects on body composition and whole-body metabolism in C57BL/6 J mice

Six months of CANA treatment had limited effects body composition. Longitudinal assessments revealed that males treated with CANA from 6 to 12 months of age (adults) weighed less than sex- and age-matched controls (treatment effect, p=.0427). CANA-treated females had less fat mass compared with age-matched controls, regardless of their age at treatment onset (treatment effect, p=.00858 for young females, $p<.0001$ for adult females).

Body weight and composition were evaluated monthly. Compared to age- and sex-matched controls, males starting CANA treatment at 6-months-of-age had lower bodyweight (Figure S9C, See online supplementary material for a color version of this figure). Changes in body composition over the course of the experiment, calculated as the difference between baseline and final measurements, revealed that CANA did not alter bodyweight or lean mass in any cohorts analyzed (Figure S9E and F, See online supplementary material for a color version of this figure). The change in fat mass and body fat percent was greater in CANA-treated males aged 6-months at treatment initiation (Fig. S9G-H, See online supplementary material for a color version of this figure). Fat mass and percent body fat was not altered by CANA treatment in females or young males.

Despite significantly lowering fasting blood glucose levels (Figure S10, See online supplementary material for a color version of this figure), 6 months of CANA treatment had few effects on whole body metabolism. At the end of the treatment period, females that started CANA at 3-months-of-age had greater nighttime energy expenditure compared with

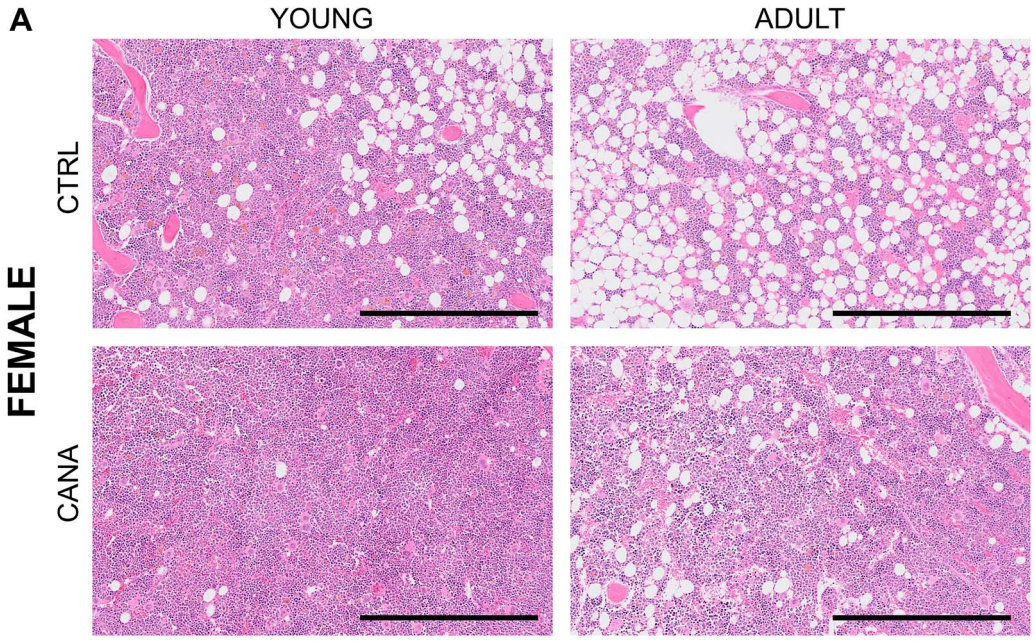

B

Bone Marrow Adiposity: Females

		Average Adipcotyes/Area (#/um^2)	Average Adipocyte Size (um^2)	Average Percent Area Covered by Adipocytes
Young	Control	24.66E-05 ± 13.68E-05	8445.09 ± 1352.34	18.91 ± 10.94
	CANA	3.52E-05 ± 1.48E-05	5137.24 ± 725.42	1.67 ± 0.76
Adult	Control	34.85E-05 ± 27.43E-05	7311.13 ± 1868.82	26.30 ± 22.56
	CANA	18.93E-05 ± 8.58E-05	6048.87 ± 1268.32	11.18 ± 7.37

Figure 6. CANA treatment reduced marrow adiposity in females. (A) Representative images of marrow adiposity; sections stained with hematoxylin and eosin. (B) Adipocyte number, size, and percent area covered were reduced by CANA treatment ($p<.05$). Age at euthanasia did not affect marrow adiposity. Scale bar = 500 μm. Abbrevation: CANA, canagliflozin.

controls (Figure S8C, See online supplementary material for a color version of this figure, 10% increase). Males starting treatment at 6-months-of-age had greater daytime energy expenditure compared with controls (Figure S8D, See online supplementary material for a color version of this figure, 10% increase). The 24-hour average respiratory exchange ratio was reduced in CANA-treated males compared with controls (4% reduction in young males and 3% in adult males). Similarly, CANA-treated males had increased the 24-hour oxygen consumption compared to age and sex-matched controls (8% increase in young males and 7% in adult males). Females beginning treatment at 3-months of age (young) had both increased oxygen consumption and carbon dioxide expulsion over a 24-hour period (5% and 1%, respectively). Nighttime activity, including wheel running and cage ambulation, did not change with CANA treatment.

Discussion

In the current study, we interrogated the effects of CANA treatment on the skeleton in the C57BL/6 J mouse, examining differences between skeletally immature (3-month-old) and mature (6-month-old) animals. CANA treatment affected the skeleton similarly in young and adult animals. Across all cohorts, CANA treatment reduced bone formation. Following CANA treatment, osteoblast number, serum P1NP and bone marrow adipocyte number were reduced in a sex-specific manner. Despite reduced bone formation, 6 months of CANA treatment conferred morphological benefits to both cortical and trabecular bone.

The increased risk of bone fracture observed in patients receiving CANA treatment is primarily driven by data collected in the initial CANVAS clinical trial[9]; non-CANVAS studies did not record increased fractures with CANA treatment.[2,10,11] Variability in CANA-associated fracture risk may be due to variation within patient populations between the CANVAS and non-CANVAS studies. All patients had type II diabetes[9] and therefore increased fracture risk compared to the general population. Although duration of diabetes was similar between the CANVAS and CREDENCE trials, treatment history could affect fracture risk.[3,28] Variation in geographical recruitment and patient ethnicity also could have contributed to differing fracture risks.[2,3,28]

Use of CANA has recently expanded to nondiabetic populations to treat cardiovascular disease,[3] but preclinical investigations into the effect of CANA on skeletal health in the absence of diabetes are limited.[22,23,29] In preclinical models, variability in CANA-induced changes to the skeleton may be driven by genetic variability and animal age. Genetic differences between mouse strains affect bone,[30,31] which could influence preclinical studies. The increased food intake of C57Bl6 mice recorded in this study could potentially lead to increased CANA dosing compared to previous analyses in UM-HET3 mice[6]; however, food intake was measured as the amount of

food removed from the hopper and could not account for shredding of food pellets, therefore, predicted doses may be greater than the true dosing. Further, the developmental stage of the animal at treatment onset affects bone morphology changes during the treatment period[32–34] as well as the cell populations within the skeleton.[35–37] Our study provides novel, direct comparisons between the developmental stage of the animal at the start of treatment, providing insight into skeletal responses both prior to and after periods of accelerated bone loss.

In nondiabetic preclinical models, the temporal response of bone to CANA may differ, reflected by differences in treatment timelines. In previous examinations of nondiabetic DBA/2 J males, short-term treatment with CANA (10 weeks) had limited effects on bone; bone volume fraction was reduced by CANA, but no changes to bone strength or systemic bone formation and resorption were recorded.[23] On the contrary, long-term CANA treatment (17 months) in nondiabetic UM-HET3 male mice negatively affected cortical but not trabecular bone morphology.[22] Female UM-HET3 mice treated with long-term CANA incurred deficits in both cortical and trabecular bone. Lifelong loss-of-function of the *Slc5a2* gene that encodes SGLT2 negatively affected bone morphology in 50-week-old males but did not change bone strength in either sex.[29] In our study, the early beneficial changes to bone mineral density recorded in B6 females contrast with reduced bone formation rates at euthanasia, following an intermediate period of CANA treatment (6 months), highlighting differences in the temporal responses to SGLT2 inhibition. Additionally, compared to control mice, CANA-treated females had greater increases in aBMD and aBMC, suggesting protective effects against age-related bone loss.

CANA treatment improved skeletal health more in females than male mice. Although we observed benefits to skeletal morphology in both sexes, more outcome measures were improved in females than males. In our study, reduced bone remodeling could have prevented the age-related bone loss typically observed in B6 mice.[32,38] Previous investigations of CANA may have been occluded by age-related bone loss in females.[22] In addition to the skeletal benefits recorded in females, marrow adiposity was reduced by CANA. Marrow adiposity is associated with worsened bone health[35,39] and changes with age in a sex-specific manner. Aging increases adiposity more in females than males,[40] therefore our euthanasia at 9- and 12-months of age may have precluded our ability to discern attenuation of marrow adiposity in males.

Although SGLT2 inhibition is often compared to caloric restriction models,[41] our data suggest that CANA treatment elicits a distinct skeletal phenotype. Previous examinations of CANA treatment in nondiabetic mice have documented reductions in body mass and increases in longevity,[6,22] supporting similarities between whole-body responses to SGLT2 inhibition and caloric restriction.[41] In our study, CANA induced limited changes to body composition whereas caloric restriction models elicit drastic effects on body weight and fat mass.[25,42] Furthermore, CANA treatment reduced marrow adiposity whereas caloric restriction consistently increases both bone marrow adipocyte size and number.[25,42,43] Energy expenditure is reduced in calorie-restricted animals[25] but was only minimally changed in this study. Finally, both in our study and in clinical populations, CANA increased caloric intake.[44]

The mechanisms driving the bone changes following CANA treatment are likely independent of kidney function. Despite increased calcium urinary excretion, no changes were recorded in systemic PTH levels, supporting previously published findings in nondiabetic CANA-treated mice.[23] Although the animals in our study were not hypoglycemic, reduced serum glucose levels with CANA may decrease glucose availability within bone cells or elicit a compensatory mechanism that changes the bioenergetic state of bone cells. Compared to other organs in the body, bone takes up a large proportion of glucose.[45] Glycolysis, which requires glucose as its primary substrate, is elevated during osteoblastic differentiation.[46–48] Runx2-mediated osteoblastic differentiation and deposition of collagen by osteoblasts is dependent on glucose availability.[49] The reductions in osteoblast number and serum P1NP measured in this study indicate that CANA negatively affects osteoblasts. Although osteoclastic resorptive activities rely on the influx of glucose as the primary substrate,[50] we recorded no differences due to CANA treatment in osteoclast number or activity, suggesting that the primary influence of CANA on bone is mediated by changes to mesenchymal progenitors.

Our study has some limitations that should be addressed in future experiments. Although we evaluated longitudinal changes to aBMD with DXA scanning, future use of in vivo μCT would allow us to confirm our hypothesis that age-related bone loss was attenuated by CANA. Despite similarities in treatment-induced changes to bone morphology between males and females, further evaluation of the mechanisms driving these changes is warranted. Another limitation of our study is the examination of only long bones (femur and tibia), so future investigations should include additional skeletal sites. In addition to changes in bone morphology, CANA treatment likely altered bone mineralization,[22] therefore, a more detailed analysis of mineral content should be evaluated in future investigations. The findings we recorded in bone marrow adiposity may not translate to other mouse strains or humans, due to the high sensitivity of C57BL6/J mice to metabolic alterations. Although CANA has been expanded to nondiabetic patient populations, our investigation did not include models that suffer from the cardiac diseases indicated for treatment. Confounding effects of these diseases on bone could lead to different skeletal changes compared to what we measured here. Finally, we cannot exclude a cell autonomous effect by which CANA might bind to other skeletal ion transporters or exchangers (e.g. sodium hydrogen exchangers) in bone cells.

In summary, we demonstrated that 6 months of CANA treatment reduced bone formation by impairing osteoblast numbers, likely due to progenitor recruitment. Despite limited changes to systemic body composition and metabolism, CANA-treated animals had improved bone morphology. In females, CANA also reduced bone marrow adiposity. Our work highlights the non-cell autonomous effects of CANA on the skeleton in nondiabetic B6 mice.

Acknowledgments

We thank Peter Caradonna for assistance with histology and Jen Daruszka for assistance with animal work.

Author contributions

Conceptualization: CC, SY, CJR. Data curation: CC, VED, SY. Formal Analysis: CC, CM, VED, SY. Investigation: CC, CM, SNC, VED, SY. Methodology: CC, SNC, SY, CJR. Project Administration: CC, SY, CJR. Resources: SY, CJR. Software: VED, SY. Supervision: SY, CJR.

Validation: CC, CM. Visualization: CC, CM. Writing—Original Draft: CC. Writing—Review & Editing: CC, CM, SNC, VED, SY, CJR.

Carolyn Chlebek (Conceptualization, Data curation, Formal analysis, Investigation, Methodology, Project administration, Validation, Visualization, Writing—original draft, Writing—review & editing), Casey McAndrews (Formal analysis, Investigation, Visualization, Writing—review & editing), Samantha Costa (Investigation, Methodology, Writing—review & editing), Victoria DeMambro (Formal analysis, Resources, Software, Writing—review & editing), Shoshana Yakar (Conceptualization, Funding acquisition, Investigation, Methodology, Resources, Software, Writing—review & editing), and Clifford Rosen (Conceptualization, Funding acquisition, Project administration, Resources, Writing—review & editing).

Supplementary material

Supplementary material is available at *JBMR Plus* online.

Funding

Financial support was received from the National Institutes of Health Grant R01AG056397 and B01 (2024) Department of Molecular Pathobiology Accelerator Award, RB841-001421 MEGA grant, and RAPID grant A22-0392 NYUCD, to SY. Histology was performed at the University of New England Histology and Imaging Core, funded by NIGMS P20GM103643.

Conflicts of interest

The authors declare no conflict of interest. All authors have read and agreed to the published version of the manuscript.

Ethics approval/institutional review board statement

The animal study protocol was approved by the Institutional Animal Care and Use Committee (IACUC) of MaineHealth Institute for Research (protocol #1914).

Data availability statement

The data that support the findings of this study are available from the corresponding author upon request.

References

1. Vallon V, Platt KA, Cunard R, et al. SGLT2 mediates glucose reabsorption in the early proximal tubule. *J Am Soc Nephrol*. 2011;22(1):104–112. https://doi.org/10.1681/ASN.2010030246
2. Zhou Z, Jardine M, Perkovic V, et al. Canagliflozin and fracture risk in individuals with type 2 diabetes: results from the CANVAS program. *Diabetologia*. 2019;62(10):1854–1867. https://doi.org/10.1007/s00125-019-4955-5
3. Neal B, Perkovic V, Mahaffey KW, et al. Canagliflozin and cardiovascular and renal events in type 2 diabetes. *N Engl J Med*. 2017;377(7):644–657. https://doi.org/10.1056/NEJMoa1611925
4. Spertus JA, Birmingham MC, Nassif M, et al. The SGLT2 inhibitor canagliflozin in heart failure: the CHIEF-HF remote, patient-centered randomized trial. *Nat Med*. 2022;28(4):809–813. https://doi.org/10.1038/s41591-022-01703-8
5. Adhikari R, Jha K, Dardari Z, et al. National trends in use of sodium-glucose cotransporter-2 inhibitors and glucagon-like peptide-1 receptor agonists by cardiologists and other specialties, 2015 to 2020. *J Am Heart Assoc*. 2022;11(9):e023811. https://doi.org/10.1161/JAHA.121.023811
6. Miller RA, Harrison DE, Allison DB, et al. Canagliflozin extends life span in genetically heterogeneous male but not female mice. *JCI Insight*. 2020;5(21):e140019. https://doi.org/10.1172/jci.insight.140019
7. Dave CV, Schneeweiss S, Wexler DJ, Brill G, Patorno E. Trends in clinical characteristics and prescribing preferences for SGLT2 inhibitors and GLP-1 receptor agonists, 2013–2018. *Diabetes Care*. 2020;43(4):921–924. https://doi.org/10.2337/dc19-1943
8. Seeman E. Age- and menopause-related bone loss compromise cortical and trabecular microstructure. *J Gerontol A Biol Sci Med Sci*. 2013;68(10):1218–1225. https://doi.org/10.1093/gerona/glt071
9. Watts NB, Bilezikian JP, Usiskin K, et al. Effects of canagliflozin on fracture risk in patients with type 2 diabetes mellitus. *J Clin Endocrinol Metab*. 2016;101(1):157–166. https://doi.org/10.1210/jc.2015-3167
10. Ko HY, Bea S, Jeong HE, et al. Sodium-glucose cotransporter 2 inhibitors vs Incretin-based drugs and risk of fractures for type 2 diabetes. *JAMA Netw Open*. 2023;6(9):e2335797. https://doi.org/10.1001/jamanetworkopen.2023.35797
11. Rigato M, Fadini GP, Avogaro A. Safety of sodium-glucose cotransporter 2 inhibitors in elderly patients with type 2 diabetes: a meta-analysis of randomized controlled trials. *Diabetes Obes Metab*. 2023;25(10):2963–2969. https://doi.org/10.1111/dom.15193
12. Wang Y, Zhou X. The relationship between use of SGLT2is and incidence of respiratory and infectious diseases and site-specific fractures: a meta-analysis based on 32 large RCTs. *Eur J Clin Pharmacol*. 2024;80(4):563–573. https://doi.org/10.1007/s00228-024-03631-7
13. Chen J, Williams S, Ho S, et al. Quantitative PCR tissue expression profiling of the human SGLT2 gene and related family members. *Diabetes Ther*. 2010;1(2):57–92. https://doi.org/10.1007/s13300-010-0006-4
14. Chlebek C, Moore JA, Ross FP, van der Meulen MCH. Molecular identification of spatially distinct anabolic responses to mechanical loading in murine cortical bone. *J Bone Miner Res*. 2022;37(11):2277–2287. https://doi.org/10.1002/jbmr.4686
15. Damasiewicz MJ, Nickolas TL. Rethinking bone disease in kidney disease. *JBMR Plus*. 2018;2(6):309–322. https://doi.org/10.1002/jbm4.10117
16. Alexander RT, Dimke H. Effect of diuretics on renal tubular transport of calcium and magnesium. *Am J Physiol-Ren Physiol*. 2017;312(6):F998–F1015. https://doi.org/10.1152/ajprenal.00032.2017
17. Alexander RT, Dimke H. Effects of parathyroid hormone on renal tubular calcium and phosphate handling. *Acta Physiol*. 2023;238(1):e13959. https://doi.org/10.1111/apha.13959
18. Blau JE, Bauman V, Conway EM, et al. Canagliflozin triggers the FGF23/1,25-dihydroxyvitamin D/PTH axis in healthy volunteers in a randomized crossover study. *JCI Insight*. 2018;3(8):e99123. https://doi.org/10.1172/jci.insight.99123
19. Sha S, Devineni D, Ghosh A, et al. Pharmacodynamic effects of canagliflozin, a sodium glucose co-transporter 2 inhibitor, from a randomized study in patients with type 2 diabetes. *PLoS One*. 2014;9(8):e105638. https://doi.org/10.1371/journal.pone.0105638
20. Iijima H, Kifuji T, Maruyama N, Inagaki N. Pharmacokinetics, pharmacodynamics, and safety of canagliflozin in Japanese patients with type 2 diabetes mellitus. *Adv Ther*. 2015;32(8):768–782. https://doi.org/10.1007/s12325-015-0234-0
21. Jackson K, Moseley KF. Diabetes and bone fragility: SGLT2 inhibitor use in the context of renal and cardiovascular benefits. *Curr Osteoporos Rep*. 2020;18(5):439–448. https://doi.org/10.1007/s11914-020-00609-z
22. Yildirim G, Bergamo ETP, Poudel SB, et al. Long-term effects of canagliflozin treatment on the skeleton of aged UM-HET3 mice. *GeroScience*. 2023;45(3):1933–1951. https://doi.org/10.1007/s11357-023-00803-8
23. Thrailkill KM, Clay Bunn R, Nyman JS, et al. SGLT2 inhibitor therapy improves blood glucose but does not prevent diabetic bone disease in diabetic DBA/2J male mice. *Bone*. 2016;82:101–107. https://doi.org/10.1016/j.bone.2015.07.025

24. DeMambro VE, Le PT, Guntur AR, et al. Igfbp2 deletion in ovariectomized mice enhances energy expenditure but accelerates bone loss. *Endocrinology*. 2015;156(11):4129–4140. https://doi.org/10.1210/en.2014-1452
25. Maridas DE, Rendina-Ruedy E, Helderman RC, et al. Progenitor recruitment and adipogenic lipolysis contribute to the anabolic actions of parathyroid hormone on the skeleton. *FASEB J*. 2019;33(2):2885–2898. https://doi.org/10.1096/fj.201800948RR
26. Bouxsein ML, Boyd SK, Christiansen BA, Guldberg RE, Jepsen KJ, Müller R. Guidelines for assessment of bone microstructure in rodents using micro–computed tomography. *J Bone Miner Res*. 2010;25(7):1468–1486. https://doi.org/10.1002/jbmr.141
27. Costa S, Fairfield H, Reagan MR. Inverse correlation between trabecular bone volume and bone marrow adipose tissue in rats treated with osteoanabolic agents. *Bone*. 2019;123:211–223. https://doi.org/10.1016/j.bone.2019.03.038
28. Perkovic V, Jardine MJ, Neal B, et al. Canagliflozin and renal outcomes in type 2 diabetes and nephropathy. *N Engl J Med*. 2019;380(24):2295–2306. https://doi.org/10.1056/NEJMoa1811744
29. Thrailkill KM, Bunn RC, Uppuganti S, et al. Genetic ablation of SGLT2 function in mice impairs tissue mineral density but does not affect fracture resistance of bone. *Bone*. 2020;133:115254. https://doi.org/10.1016/j.bone.2020.115254
30. Papageorgiou M, Föger-Samwald U, Wahl K, Kerschan-Schindl K, Pietschmann P. Age- and strain-related differences in bone microstructure and body composition during development in inbred male mouse strains. *Calcif Tissue Int*. 2020;106(4):431–443. https://doi.org/10.1007/s00223-019-00652-8
31. Rosen CJ, Dimai HP, Vereault D, et al. Circulating and skeletal insulin-like growth factor-I (IGF-i) concentrations in two inbred strains of mice with different bone mineral densities. *Bone*. 1997;21(3):217–223. https://doi.org/10.1016/S8756-3282(97)00143-9
32. Glatt V, Canalis E, Stadmeyer L, Bouxsein ML. Age-related changes in trabecular architecture differ in female and male C57BL/6J mice. *J Bone Miner Res*. 2007;22(8):1197–1207. https://doi.org/10.1359/jbmr.070507
33. Somerville JM, Aspden RM, Armour KE, Armour KJ, Reid DM. Growth of C57Bl/6 mice and the material and mechanical properties of cortical bone from the tibia. *Calcif Tissue Int*. 2004;74(5):469–475. https://doi.org/10.1007/s00223-003-0101-x
34. Flurkey K, Mcurrer J, Harrison D. Mouse models in aging research. In: Fox JG, Davisson MT, Quimby FW, Barthold SW, Newcomer CE, Smith AL (eds.) *The Mouse in Biomedical Research, American College of Laboratory Animal Medicine*. Vol III. Elsevier; 2007: 637–672. https://doi.org/10.1016/B978-012369454-6/50074-1.
35. Justesen J, Stenderup K, Ebbesen EN, Mosekilde L, Steiniche T, Kassem M. Adipocyte tissue volume in bone marrow is increased with aging and in patients with osteoporosis. *Biogerontology*. 2001;2(3):165–171. https://doi.org/10.1023/a:1011513223894
36. Perkins SL, Gibbons R, Kling S, Kahn AJ. Age-related bone loss in mice is associated with an increased osteoclast progenitor pool. *Bone*. 1994;15(1):65–72. https://doi.org/10.1016/8756-3282(94)90893-1
37. Silbermann M, Weiss A, Reznick AZ, Eilam Y, Szydel N, Gershon D. Age-related trend for osteopenia in femurs of female C57Bl/6 mice. *Compr Gerontol [A]*. 1987;1(1):45–51.
38. Ferguson VL, Ayers RA, Bateman TA, Simske SJ. Bone development and age-related bone loss in male C57BL/6J mice. *Bone*. 2003;33(3):387–398. https://doi.org/10.1016/S8756-3282(03)00199-6
39. Pino AM, Miranda M, Figueroa C, Rodríguez JP, Rosen CJ. Qualitative aspects of bone marrow adiposity in osteoporosis. *Front Endocrinol*. 2016;7:139. https://doi.org/10.3389/fendo.2016.00139
40. Griffith JF, Yeung DKW, Ma HT, Leung JCS, Kwok TCY, Leung PC. Bone marrow fat content in the elderly: a reversal of sex difference seen in younger subjects. *J Magn Reson Imaging*. 2012;36(1):225–230. https://doi.org/10.1002/jmri.23619
41. Hoong CWS, Chua MWJ. SGLT2 inhibitors as calorie restriction Mimetics: insights on longevity pathways and age-related diseases. *Endocrinology*. 2021;162(8):1–20. https://doi.org/10.1210/endocr/bqab079
42. Devlin MJ, Cloutier AM, Thomas NA, et al. Caloric restriction leads to high marrow adiposity and low bone mass in growing mice. *J Bone Miner Res*. 2010;25(9):2078–2088. https://doi.org/10.1002/jbmr.82
43. Aaron N, Kraakman MJ, Zhou Q, et al. Adipsin promotes bone marrow adiposity by priming mesenchymal stem cells. *elife*. 2021;10:e69209. https://doi.org/10.7554/eLife.69209
44. Matsuba I, Kanamori A, Takihata M, et al. Canagliflozin increases calorie intake in type 2 diabetes without changing the energy ratio of the three macronutrients: CANA-K study. *Diabetes Technol Ther*. 2020;22(3):228–234. https://doi.org/10.1089/dia.2019.0372
45. Zoch ML, Abou DS, Clemens TL, Thorek DLJ, Riddle RC. In vivo radiometric analysis of glucose uptake and distribution in mouse bone. *Bone Res*. 2016;4(1):16004. https://doi.org/10.1038/boneres.2016.4
46. Komarova SV, Ataullakhanov FI, Globus RK. Bioenergetics and mitochondrial transmembrane potential during differentiation of cultured osteoblasts. *Am J Physiol-Cell Physiol*. 2000;279(4):C1220–C1229. https://doi.org/10.1152/ajpcell.2000.279.4.C1220
47. Guntur AR, Le PT, Farber CR, Rosen CJ. Bioenergetics during calvarial osteoblast differentiation reflect strain differences in bone mass. *Endocrinology*. 2014;155(5):1589–1595. https://doi.org/10.1210/en.2013-1974
48. Schilling K, Brown E, Zhang X. NAD(P)H autofluorescence lifetime imaging enables single cell analyses of cellular metabolism of osteoblasts in vitro and in vivo via two-photon microscopy. *Bone*. 2022;154:116257. https://doi.org/10.1016/j.bone.2021.116257
49. Wei J, Shimazu J, Makinistoglu MP, et al. Glucose uptake and Runx2 synergize to orchestrate osteoblast differentiation and bone formation. *Cell*. 2015;161(7):1576–1591. https://doi.org/10.1016/j.cell.2015.05.029
50. Taubmann J, Krishnacoumar B, Böhm C, et al. Metabolic reprogramming of osteoclasts represents a therapeutic target during the treatment of osteoporosis. *Sci Rep*. 2020;10(1):21020. https://doi.org/10.1038/s41598-020-77892-4